Spin freezing by Anderson localization in one-dimensional semiconductors

C. Echeverría-Arrondo
Department of Physical Chemistry, Universidad del País Vasco UPV/EHU, E-48080 Bilbao, Spain

E. Ya. Sherman
Department of Physical Chemistry, Universidad del País Vasco UPV/EHU, E-48080 Bilbao, Spain and
IKERBASQUE Basque Foundation for Science, E-48011 Bibao, Bizkaia, Spain

(Received 5 December 2011; published 24 February 2012)

One-dimensional quantum wires are considered as prospective elements for spin transport and manipulation in spintronics. We study spin dynamics in semiconductor GaAs-like nanowires with disorder and spin-orbit interaction by using a rotation in the spin subspace gauging away the spin-orbit field. If the disorder is sufficiently strong, the spin density after a relatively short relaxation time reaches a plateau. This effect is a manifestation of the Anderson localization and depends in a universal way on the disorder and the spin-orbit coupling strength. As a result, at a given disorder, semiconductor nanowires can permit a long-term spin polarization tunable with the spin-orbit interactions.

DOI: 10.1103/PhysRevB.85.085430 PACS number(s): 72.25.Rb, 72.70.+m, 78.47.−p

I. INTRODUCTION

The main idea of spintronics—the design and application of devices controlling not only the charge dynamics but also the electron-spin evolution—can be useful for information storage, transfer, and manipulation technologies.[1–3] Possible realizations of spintronics devices can be based on semiconductor nanowires[4–10] for quasiballistic electron transport, coherent transmission of information, and spin control. These systems attract a great deal of attention due to a clear interplay of transport and spin-orbit (SO) coupling physics.[11–16]

This control faces the problem of inevitable spin relaxation due to the coupling of electron spin to environment through SO coupling. As a result, the factors determining the spin relaxation rate become of crucial importance. Two limiting cases of spin relaxation are well understood. For the itinerant electrons, spin relaxation in mainly determined by the Dyakonov-Perel mechanism, that is by random precession of electron spin due to the random in time electron momentum.

A different approach should be applied for electrons localized in a regular external potential forming quantum dots promising for quantum information applications.[17] Here momentum is not a well-defined quantity, and the momentum-dependent splitting required for the Dyakonov-Perel mechanism vanishes. In this case inelastic spin relaxation due to SO coupling occurs via phonon-induced transition between orbital states in external magnetic field.[18] In the absence of magnetic field and spin-orbit coupling, spin relaxation can occur due to the hyperfine coupling of electron spin to spins of lattice nuclei.[19] In both cases, the initial spin polarization goes asymptotically to zero. The characteristic timescale of spin relaxation of electrons localized in quantum dots is expected to be several orders of magnitude longer than that of itinerant electrons.

While these two limits of free and strongly localized electrons are well understood, the interplay of disorder-induced localization and spin relaxation of itinerant electrons remains an open question, although some aspects of the problem have been addressed.[20–23] The questions here are (i) how the localization forms the spin relaxation, and (ii) whether the initially prepared spin density relaxes to zero. As a nontrivial example of this interplay, we mention that weak localization of two-dimensional electrons leads to a long powerlike rather than exponential spin relaxation.[24,25] Here we analyze this problem for the one-dimensional system, providing, on one hand, the basic example of localization physics in a random potential,[26,27] and, on the other hand, an example of a system where spin-orbit coupling can be gauged away by a SU(2) transformation.

This paper is organized as follows. In Sec. II, we show how to treat spin relaxation in one-dimensional systems with the gauge transformation and introduce the tight-binding Hamiltonian for the model. The spin dynamics will be analyzed by a numerically exact calculation in Sec. III, where we show that spin density does not relax to zero, in contrast to what is expected. In addition, in Sec. III, we study how asymptotic value of spin polarization depends on the disorder and spin-orbit coupling. Conclusions summarize the results in Sec. IV.

II. MODEL

A. Hamiltonian and gauge transformation

The investigated structure is a quantum wire extended along the x axis, as shown in Fig. 1. The total Hamiltonian has the form

$$\hat{H} = \frac{\hbar^2}{2m}(k_x - A_x)^2 + U(x) - \frac{m\alpha^2}{2\hbar^2}, \tag{1}$$

where $A_x = -m\alpha\sigma_y/\hbar^2$ stands for the Rashba coupling[28] with strength α, σ_y is the Pauli matrix, k_x is the electron wavevector, and m is the effective mass. The Dresselhaus coupling[29] is obtained with $A_x = -m\beta\sigma_x/\hbar^2$, where β is the coupling constant. Without loss of generality, we concentrate here on the Rashba coupling, which can be changed on demand by applying an external electric field across the structure.[30]

The SO interaction can be removed from $\hat{H}$ in Eq. (1) through a gauge transformation[31,32] with a SU(2) spin

 ©2012 American Physical Society

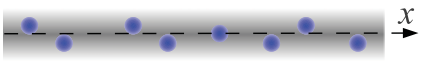

FIG. 1. (Color online) Semiconductor nanowire with random impurities shown as filled circles. Although we consider a one-dimensional electron motion, impurities can be randomly distributed over the crosssection of the wire.

rotation: $\hat{S} = \exp\left(-ix\sigma_y/2\xi\right)$, where $\xi = \hbar^2/2m\alpha$ is the spin-precession length. After this transformation, the system Hamiltonian has the form: $\hat{\tilde{H}} = \hbar^2 k_x^2/2m + U(x)$.

Since for the Hamiltonian (1) σ_y is the integral of motion, the spin density component along the y axis is time independent. A nontrivial dynamics of the transformed spin occurs for the $\gamma = (x,z)$ spin components $\langle \tilde{s}_\gamma(x,t)\rangle$ and can be expressed in terms of the spin diffusion

$$\langle \tilde{s}_\gamma(x,t)\rangle = \int D^{\gamma\beta}(x-x',t)\langle \tilde{s}_\beta(x',0)\rangle dx', \tag{2}$$

where $D^{\gamma\beta}(x,t)$ is the exact disorder-dependent one-dimensional spin diffusion Green's function. In a nonmagnetic system without SO coupling, $D^{\gamma\beta}(x,t) = \delta_{\gamma\beta}D(x,t)$ is diagonal in the spin subspace. As a result of the gauge transformation, the uniform density dynamics is determined by the Fourier component[25]

$$D(q,t) = \int_{-\infty}^{\infty} dx e^{-iqx} D(x,t) \tag{3}$$

with $q = 1/2\xi$, and Eq. (2) simplifies for the physical measurable spins as $\langle s_\gamma(t)\rangle = \langle s_\gamma(0)\rangle D(1/2\xi,t)$. Here we will use a similar, however, somewhat different approach based on numerically exact analysis of the direct time evolution of the initial spin-polarized states. It will be shown that the resulting spin dynamics has unexpected features, including a long-time plateau in the spin polarization.

The eigenfunctions of $\hat{\tilde{H}}$ can be taken in the form $\overline{\psi}(x) = \psi(x)|1\rangle$ and $\overline{\psi}(x) = \psi(x)|-1\rangle$, where $|\pm 1\rangle$ are the eigenstates of σ_z with the corresponding eigenvalues. The eigenstates of $\hat{H}$, $\overline{\phi}(x)$, can be obtained by spin rotation of the $\overline{\psi}(x)|\sigma\rangle$ states. For example, with spin-up initial state $\overline{\psi}(x)|1\rangle$, one obtains

$$\overline{\phi}(x) = \psi(x)\left[\cos\left(\frac{x}{2\xi}\right)|1\rangle + \sin\left(\frac{x}{2\xi}\right)|-1\rangle\right]. \tag{4}$$

The spin dynamics and spin relaxation in the system, as will be shown below, are solely due to the entanglement of spin and coordinate in Eq. (4).

B. Tight-binding model and disorder

We perform numerical analysis using the tight-binding model, employing the approach similar to Refs. 16 and 33. The one-dimensional electron gas is sampled with $N = 2^{13}$ (8192) grid points $x_n = nl$, where $1 \leqslant n \leqslant N$, and l is the effective lattice constant with periodic boundary conditions.[34] The effective hopping matrix element between two nearest neighbors is chosen as $t = 50$ meV, and the kinetic energy is $E(k_x) = 2t[1-\cos(k_x l)]$. The eigenenergies span the range 0–200 meVs. The distance between two neighbor grid points becomes $l = \hbar/\sqrt{2mt} = 3.37$ nm to satisfy the electron effective mass $m = 0.067m_0$ in a GaAs semiconductor, with m_0 being the free electron mass.

The random potential $U_n = U(x_n)$ uniformly spans the range $[-U_0/2, U_0/2]$, with the white noise correlator $\langle U(x_{n_1})U(x_{n_2})\rangle = \langle U^2\rangle\delta_{n_1,n_2}$, where $\langle U^2\rangle = U_0^2/12$. The effects of disorder can be approximately characterized through the energy-dependent momentum relaxation time τ_E, which we define as $\hbar/\tau_E = \langle U^2\rangle l \nu_E$, where $\nu_E = \sqrt{m}/\pi\hbar\sqrt{2E}$ is the density of states per spin component. The resulting mean free path is $\ell_E = v_E\tau_E$, where $v_E = \sqrt{2E/m}$ is the electron speed, and the corresponding diffusion coefficient is $D_E = v_E^2\tau_E$.

In this representation, the eigenstates of $\hat{\tilde{H}}$ and $\hat{H}$ form basis sets, $\{\overline{\psi}_i\}$ and $\{\overline{\phi}_i\}$ respectively, where $1 \leqslant i \leqslant 2N$. For the same i, these two sets are related by the local spin rotation $\hat{S}$. We assume that $\overline{\psi}_i = \psi_i(x_n)|1\rangle$ for $1 \leqslant i \leqslant N$, and $\overline{\psi}_i = \psi_{i-N}(x_n)|-1\rangle$ for $N < i \leqslant 2N$.

III. SPIN DYNAMICS

We study dynamics of initial $\overline{\psi}_i$ states with $1 \leqslant i \leqslant N$, corresponding to the evolution after switching on the SO coupling. The time dependence can be expressed with the spectral decomposition as:

$$\overline{\psi}_j^{\rm so}(t) = \sum_{i=1,2N} a_{ij}\overline{\phi}_i e^{-it\varepsilon_i/\hbar}, \tag{5}$$

where $a_{ij} = \langle\overline{\phi}_i|\overline{\psi}_j\rangle$, and ε_i are the corresponding eigenenergies. The spin component expectation value $\langle\sigma_z(t)\rangle_j = \langle\overline{\psi}_j^{\rm so}(t)|\sigma_z|\overline{\psi}_j^{\rm so}(t)\rangle$ is determined by the spectrum and eigenstates of the system.

In order to give an idea of the entanglement induced by SO coupling, we present in Fig. 2 the evolution of the $\overline{\phi}_{N/4}(x_n)$ state with the increase in spin-orbit coupling. At $\alpha = 0$, we obtain a product state $\overline{\phi}_{N/4}(x_n) = \psi_{N/4}(x_n)|1\rangle$, and with the increase in α, entangled states are formed. The overlap of $\overline{\phi}_i(x_n)$ and $\overline{\psi}_j(x_n)$ eigenstates is characterized by two sets of matrix elements a_{ij}; for example, for $1 \leqslant j \leqslant N$:

$$\begin{aligned} a_{ij} &= \sum_n \cos\left(\frac{x_n}{2\xi}\right)\psi_i(x_n)\psi_j(x_n), \quad 1 \leqslant i \leqslant N, \\ a_{ij} &= \sum_n \sin\left(\frac{x_n}{2\xi}\right)\psi_i(x_n)\psi_j(x_n), \quad N < i \leqslant 2N. \end{aligned} \tag{6}$$

The behavior of a_{ij} presented in Fig. 3 demonstrates that for a given j, it has nonnegligible values only in a certain, rather narrow, range of i.

To illustrate the role of the random potential, we consider as examples weak ($U_0 = 15$ meV, $U_0 \ll t$) and strong ($U_0 = 55$ meV, $U_0 > t$) disorder. For free electrons in state $j = N/4$ and $E = 31$ meV, the resulting $\hbar/\tau_E$ is about 0.1 and 1 meV, respectively. For a free electron with energy $E \approx 20$ meV, the velocity is $v_E \approx 3.5 \times 10^7$ cm/s, the mean free path is $\ell_E \sim 2.5 \times 10^{-5}$ cm ($\hbar/\tau_E = 1$ meV), and the corresponding diffusion coefficient is $D_E \sim 10^3$ cm^2/s. These parameters provide an effective integral characteristic of the disorder and correspond to realistic parameters of the wires, which,

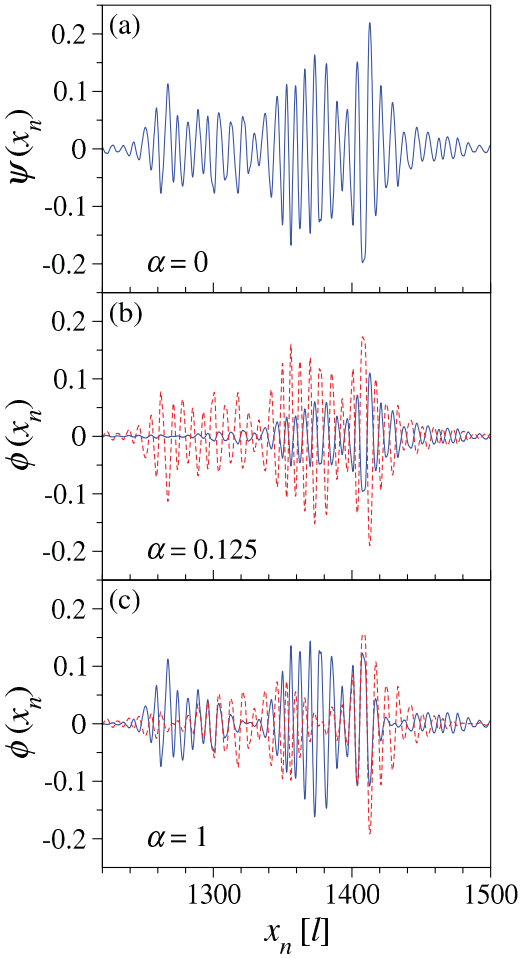

FIG. 2. (Color online) Site dependent components of $\overline{\phi}_{N/4}(x_n)$ for a qualitative description of entanglement induced by the gauge transformation for (a) $\alpha = 0$, (b) $\alpha = 0.125 \times 10^{-6}$ meV cm, and (c) $\alpha = 10^{-6}$ meV cm ($U_0 = 55$ meV). The solid and dashed lines represent $|1\rangle$ and $|-1\rangle$ components, respectively.

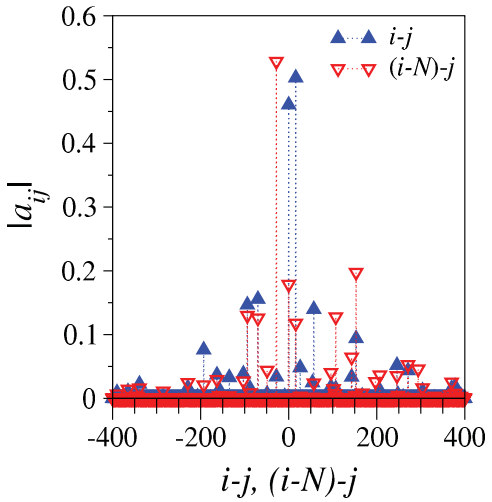

FIG. 3. (Color online) Absolute values of a_{ij} around the initial spin-up state $\overline{\psi}_{N/4}$; here $\alpha = 10^{-6}$ meV cm (strong SO coupling) and $U_0 = 55$ meV (strong disorder).

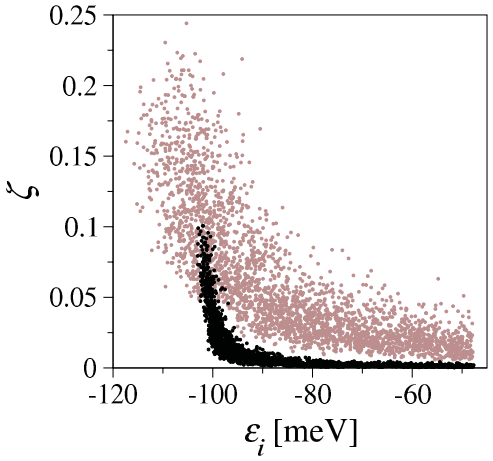

FIG. 4. (Color online) Inverse participation ratio ζ for the low part of the energy spectrum; gray circles denote strong disorder ($U_0 = 55$ meV), and black circles denote weak disorder ($U_0 = 15$ meV). Since even for $U_0 = 55$ meV we obtain $\zeta \ll 1$, the localized states spread over many lattice sites, confirming applicability of the tight-binding Hamiltonian for the localization problem.

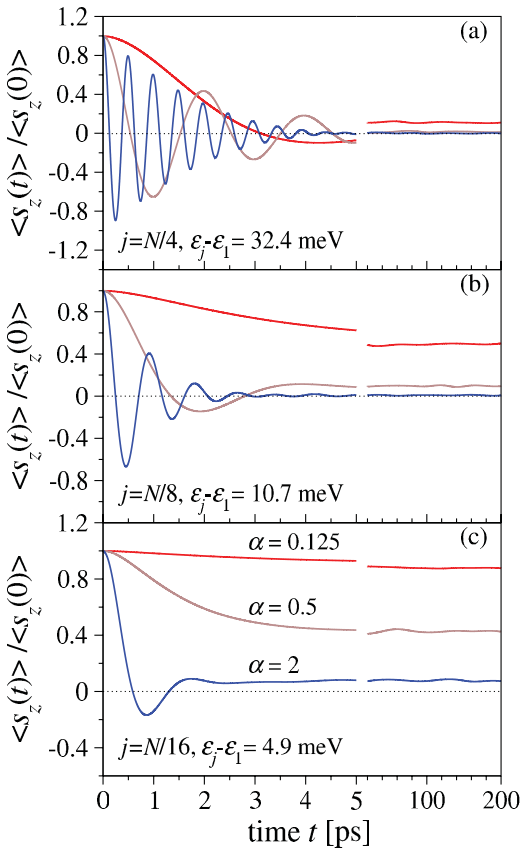

FIG. 5. (Color online) Time-dependent polarization in the weak-disorder regime ($U_0 = 15$ meV). The initial bins are centered at the states (a) $N/4$ (bin width 6.8 meV), (b) $N/8$ (bin width 3.7 meV), and (c) $N/16$ (bin width 2.1 meV) with energies decreasing in the same order. The order of plots in all panels is as marked in panel (c) for SO coupling strengths in units of 10^{-6} meVcm. Note that after the relaxation stage, the spin density remains a finite constant.

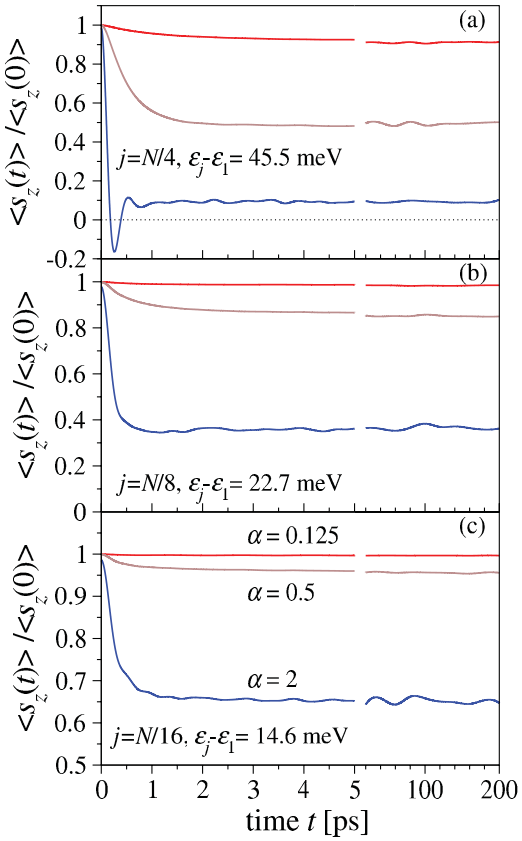

FIG. 6. (Color online) Time-dependent spin polarization in the strong-disorder regime ($U_0 = 55$ meV) with the same notations as in Fig. 5. (a) $N/4$ (bin width 7.2 meV), (b) $N/8$ (bin width 4.5 meV), and (c) $N/16$ (bin width 3.7 meV). Note that for $\alpha = 0.125 \times 10^{-6}$ meVcm the spin is almost constant in time, thus suitable for spin-based operations.

however, can strongly vary from sample to sample and from experiment to experiment.

The effect of localization by disorder is seen in the inverse participation ratio[35] (IPR) $\zeta_i = \sum_n |\psi_i^4(x_n)|$. The IPR calculated for the low-energy spectrum is presented in Fig. 4. As expected, the degree of localization increases with U_0, and this effect is more pronounced for the electrons with lowest energies. In contrast to the results of Ref. 23, the IPR in this system does not depend on the SO coupling. We now study the effects of disorder and spin-orbit coupling on the average spin dynamics of a bin of 256 initial spin-up states and eight realizations of the random potential. The statistical error of this approach is therefore $1/\sqrt{2048} = 2.2\%$, making the results statistically representative.

We take three example bins with three different degrees of localization. The bins are centered around the spin-up states $\overline{\psi}_{N/4}$, $\overline{\psi}_{N/8}$, and $\overline{\psi}_{N/16}$, whose IPR values increase in the same order (energies decreasing, see Fig. 4). The calculated bin- and potential realization-averaged spin dynamics is shown in Figs. 5 and 6, revealing strong influence of the disorder-induced spatial localization of states. Physically, collisions of electrons with impurities force electron spin to frequently reverse the precession direction. In the classical picture, this leads to a long Dyakonov-Perel spin relaxation. If the quantum

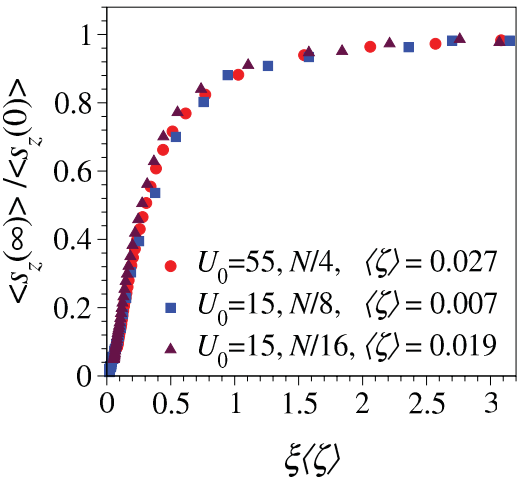

FIG. 7. (Color online) Long-term relative polarization as a function of $\xi\langle\zeta\rangle$ for three different degrees of localization. Parameter ξ is modified by changing the coupling constant α.

effects of localization are important, one observes "freezing" of the spin density. As one can see in Figs. 5 and 6, the electron-spin density relaxes for $\simeq$5 ps and then remains constant in time for infinitely long (beyond 0.2 ns in our computation). As expected, the spin polarization plateau is higher (i) for localized states and (ii) for weak SO interaction. Almost time-independent spin states are achieved, e.g., at $U_0 = 55$ meV and $\alpha = 0.125 \times 10^{-6}$ meV cm.

To gain insight into the problem, we study the dependence of asymptotic spin density on SO coupling and the localization of electrons in more detail. The long-term densities are plotted in Fig. 7 against parameter $\xi\langle\zeta\rangle$. This parameter combines the two factors determining the spin dynamics, SO coupling and spatial localization, where $\langle\zeta\rangle$ is averaged over 256 bin states and eight realizations of the random potential. The given values follow a universal dependence indicating a unique trend for long-term spins against SO coupling and localization through disorder. This trend corresponds to a fast increase in the asymptotic steady polarization for $\xi\langle\zeta\rangle < 1$ and a smooth increase and saturation for $\xi\langle\zeta\rangle > 1$. These results can be understood as follows. To show an efficient spin dynamics, the electron should move the distance of the order of $\pi\xi$. Therefore, the spatial spread of the corresponding states should be larger than $\pi\xi$. With a stronger localization, the spread and the overlap decrease, leading to the universal behavior shown in Fig. 7. Qualitatively, in the "clean" $\xi\langle\zeta\rangle \ll 1$ regime,[36] the spin relaxation has the Dyakonov-Perel mechanism either purely exponential for $\Omega_E\tau_E \ll 1$ or a combination of oscillations and exponential decay if $\Omega_E\tau_E \geqslant 1$, where the spin precession rate $\Omega_E = 2\alpha\sqrt{2mE}/\hbar$ corresponds to the electron momentum at given energy E.

IV. CONCLUSION

To summarize, localization effects of disorder and spin-orbit coupling in semiconductor nanowires determine the dynamics of electronic spins. Our tight-binding model calculations show that a prepared spin density relaxes until

reaching a plateau, directly related to the disorder and strength of spin-orbit interaction. In contrast to the expected decay to zero, a long-time constant polarization plateau survives to infinite time. The asymptotic spin density has a universal dependence on the product of the inverse participation ratio and the spin precession length. In the absence of magnetic field, the hyperfine coupling to the spins of nuclei will lead to spin relaxation on timescales at least two orders of magnitude longer than the timescale of the plateau formation of the order of 10 ps.[19] As the experiments on spin transport did not reveal electron-electron interaction effects,[8] here we have neglected them. Furthermore, whether there exists a range of parameters where the Coulomb forces can be strong enough to modify our results for localized states, remains to be investigated.

An immediate consequence of this result is the ability, by choosing the desired Rashba SO parameter for a given wire, to produce and destroy steady spin states, which are of interest for spin-based operations. These results suggest that semiconductor nanowires can be used for coherent transmission and storage of information, manipulated by spatially and temporally modulated spin-orbit coupling.

ACKNOWLEDGMENTS

We thank G. Japaridze, J. Siewert, R. Winkler, and L.-A. Wu for helpful discussions. This work was supported by the UPV/EHU under program UFI 11/55, the MCI of Spain Grant No. FIS2009-12773-C02-01 and "Grupos Consolidados UPV/EHU del Gobierno Vasco" Grant No. IT-472-10.

[1] I. Zutić, J. Fabian, and S. Das Sarma, Rev. Mod. Phys. **76**, 323 (2004); J. Fabian, A. Matos-Abiague, C. Ertler, P. Stano, and I. Zutic, Acta Physica Slovaca **57**, 565 (2007).
[2] A. Fert, Rev. Mod. Phys. **80**, 1517 (2008).
[3] M. W. Wu, J. H. Jiang, and M. Q. Weng, Phys. Rep. **493**, 61 (2010).
[4] X. Duan, Y. Huang, Y. Cui, J. Wang, and C. M. Lieber, Nature (London) **409**, 66 (2001).
[5] S. Nadj-Perge, S. Frolov, E. Bakkers, and L. Kouwenhoven, Nature (London) **468**, 1084 (2010).
[6] S. Pramanik, S. Bandyopadhyay, and M. Cahay, Phys. Rev. B **68**, 075313 (2003).
[7] A. A. Kiselev and K. W. Kim, Phys. Rev. B **61**, 13115 (2000).
[8] C. H. L. Quay, T. L. Hughes, J. A. Sulpizio, L. N. Pfeiffer, K. W. Baldwin, K. W. West, D. Goldhaber-Gordon, and R. de Picciotto, Nat. Phys. **6**, 336 (2010).
[9] A. Bringer and T. Schäpers, Phys. Rev. B **83**, 115305 (2011).
[10] M. Governale and U. Zülicke, Phys. Rev. B **66**, 073311 (2002).
[11] Y. V. Pershin, J. A. Nesteroff, and V. Privman, Phys. Rev. B **69**, 121306 (2004); V. A. Slipko, I. Savran, and Y. V. Pershin, *ibid.* **83**, 193302 (2011).
[12] A. W. Holleitner, V. Sih, R. C. Myers, A. C. Gossard, and D. D. Awschalom, Phys. Rev. Lett. **97**, 036805 (2006).
[13] M. M. Gelabert, L. Serra, D. Sánchez, and R. López, Phys. Rev. B **81**, 165317 (2010); D. Sánchez, L. Serra, and M.-S. Choi, *ibid.* **77**, 035315 (2008).
[14] C. Lü, U. Zülicke, and M. W. Wu, Phys. Rev. B **78**, 165321 (2008).
[15] C. L. Romano, P. I. Tamborenea, and S. E. Ulloa, Phys. Rev. B **74**, 155433 (2006)
[16] G. I. Japaridze, H. Johannesson, and A. Ferraz, Phys. Rev. B **80**, 041308 (2009); M. Malard, I. Grusha, G. I. Japaridze, and H. Johannesson, *ibid.* **84**, 075466 (2011).
[17] G. Burkard, D. Loss, and D. P. DiVincenzo, Phys. Rev. B **59**, 2070 (1999); L.-A. Wu and D. A. Lidar, Phys. Rev. Lett. **91**, 097904 (2003); L.-A. Wu, D. A. Lidar, and M. Friesen, *ibid.* **93**, 030501 (2004).
[18] P. Stano and J. Fabian, Phys. Rev. Lett. **96**, 186602 (2006); Phys. Rev. B **74**, 045320 (2006).
[19] I. A. Merkulov, Al. L. Efros, and M. Rosen, Phys. Rev. B **65**, 205309 (2002).
[20] T. P. Pareek and P. Bruno, Phys. Rev. B **65**, 241305 (2002).
[21] B. I. Shklovskii, Phys. Rev. B **73**, 193201 (2006).
[22] T. Kaneko, M. Koshino, and T. Ando, Physica E **40**, 383 (2007).
[23] G. A. Intronati, P. I. Tamborenea, D. Weinmann, and R. A. Jalabert, Phys. Rev. Lett. **108**, 016601 (2012).
[24] I. S. Lyubinskiy and V. Yu. Kachorovskii, Phys. Rev. B **70**, 205335 (2004).
[25] I. V. Tokatly and E. Ya. Sherman, Phys. Rev. B **82**, 161305 (2010).
[26] P. W. Anderson, D. J. Thouless, E. Abrahams, and D. S. Fisher, Phys. Rev. B **22**, 3519 (1980).
[27] I. M. Lifshitz, S. A. Gredeskul, and L. A. Pastur, *Introduction to the Theory of Disordered Systems* (Wiley, NY, 1988); A. L. Efros and B. I. Shklovskii, *Electronic Properties of Doped Semiconductors* (Springer, Heidelberg, 1989).
[28] Yu. A. Bychkov and E. I. Rashba, JETP Lett. **39**, 79 (1984).
[29] G. Dresselhaus, Phys. Rev. **100**, 580 (1955).
[30] D. Grundler, Phys. Rev. Lett. **84**, 6074 (2000); O. Z. Karimov, G. H. John, R. T. Harley, W. H. Lau, M. E. Flatte, M. Henini, and R. Airey, *ibid.* **91**, 246601 (2003); A. Balocchi, Q. H. Duong, P. Renucci, B. L. Liu, C. Fontaine, T. Amand, D. Lagarde, and X. Marie, *ibid.* **107**, 136604 (2011).
[31] L. S. Levitov and E. I. Rashba, Phys. Rev. B **67**, 115324 (2003).
[32] I. Tokatly and E. Ya. Sherman, Ann. Phys. **325**, 1104 (2010).
[33] E. M. Hankiewicz, L. W. Molenkamp, T. Jungwirth, and J. Sinova, Phys. Rev. B **70**, 241301 (2004).
[34] Since we are studying the spin dynamics in the lower part of the spectrum, the matrix Hamiltonian is only partially diagonalized up to 2800 eigenenergies and eigenstates. We use for this purpose the Lanczos method as implemented in the PARPACK package, a collection of Fortran routines for parallel computing. See [www.caam.rice.edu/software/ARPACK/index.html] for more information about the parallel version of ARPACK.
[35] F. Evers and A. D. Mirlin, Phys. Rev. Lett. **84**, 3690 (2000).
[36] V. N. Gridnev, Pis'ma Zh. Eksp. Teor. Fiz. **74**, 417 (2001) [V. N. Gridnev, JETP Lett. **74**, 380 (2001)]; C. Grimaldi, Phys. Rev. B **72**, 075307 (2005); M. M. Glazov, Solid State Commun. **142**, 531 (2007); X. Liu, X.-J. Liu, and J. Sinova, Phys. Rev. B **84**, 035318 (2011).